

Accepted Manuscript

A new Suzuki synthesis of triphenylethylenes that inhibit aromatase and bind to estrogen receptors α and β

Li-Ming Zhao, Hai-Shan Jin, Jinzhong Liu, Todd C. Skaar, Joseph Ipe, Wei Lv, David A. Flockhart, Mark Cushman

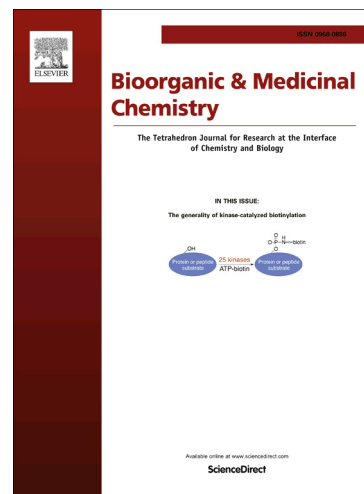
PII: S0968-0896(16)30681-2
DOI: <http://dx.doi.org/10.1016/j.bmc.2016.08.064>
Reference: BMC 13247

To appear in: *Bioorganic & Medicinal Chemistry*

Received Date: 10 July 2016
Revised Date: 25 August 2016
Accepted Date: 29 August 2016

Please cite this article as: Zhao, L-M., Jin, H-S., Liu, J., Skaar, T.C., Ipe, J., Lv, W., Flockhart, D.A., Cushman, M., A new Suzuki synthesis of triphenylethylenes that inhibit aromatase and bind to estrogen receptors α and β , *Bioorganic & Medicinal Chemistry* (2016), doi: <http://dx.doi.org/10.1016/j.bmc.2016.08.064>

This is a PDF file of an unedited manuscript that has been accepted for publication. As a service to our customers we are providing this early version of the manuscript. The manuscript will undergo copyediting, typesetting, and review of the resulting proof before it is published in its final form. Please note that during the production process errors may be discovered which could affect the content, and all legal disclaimers that apply to the journal pertain.



**A new Suzuki synthesis of triphenylethylenes that inhibit aromatase and bind to
estrogen receptors α and β**

Li-Ming Zhao,^{†‡} Hai-Shan Jin,^{†‡} Jinzhong Liu,[§] Todd C. Skaar,[§] Joseph Ipe,[§] Wei Lv,[†]
David A. Flockhart,[§] and Mark Cushman^{†,*}

[†]*Department of Medicinal Chemistry and Molecular Pharmacology, College of Pharmacy, and
The Purdue University Center for Cancer Research, Purdue University, 575 Stadium Mall Drive,
West Lafayette, Indiana 47907, United States*

[‡]*School of Chemistry and Chemical Engineering, and Jiangsu Key Laboratory of Green Synthetic
Chemistry for Functional Materials, Jiangsu Normal University, Xuzhou 221116, Jiangsu, China*

[§]*Division of Clinical Pharmacology, Department of Medicine, Indiana University School of
Medicine, Indiana Institute for Personalized Medicine, Indianapolis, Indiana 46202,
United States*

1. Abstract

The design and synthesis of dual aromatase inhibitors/selective estrogen receptor modulators (AI/SERMs) is an attractive strategy for the discovery of new breast cancer therapeutic agents. Previous efforts led to the preparation of norendoxifen (**4**) derivatives with dual aromatase inhibitory activity and estrogen receptor binding activity. In the present study, some of the structural features of the potent AI letrozole were incorporated into the lead compound (norendoxifen) to afford a series of new dual AI/SERM agents based on a symmetrical diphenylmethylene substructure that eliminates the problem of E,Z isomerization encountered with norendoxifen-based AI/SERMs. Compound **12d** had good aromatase inhibitory activity ($IC_{50} = 62.2$ nM) while also exhibiting good binding activity to both ER- α ($EC_{50} = 72.1$ nM) and ER- β ($EC_{50} = 70.8$ nM). In addition, a new synthesis was devised for the preparation of norendoxifen and its analogues through a bis-Suzuki coupling strategy.

2. Introduction

In spite of considerable therapeutic advances, breast cancer remains a significant public health problem.¹ Estrogens play a prominent role in stimulating the growth and development of the majority of breast cancers.^{2,3} Hence, estrogen receptors (ERs) are important targets for the development of new therapeutic agents for breast cancer treatment. Selective estrogen receptor modulators (SERMs), which were developed in the late 1950's and early 1960's, are widely used for the treatment of breast cancer.⁴ SERMs are able to bind to the estrogen receptors (ER- α and ER- β) in much the same way as estrogens do, and they block ERs in breast cancer cells in breast tissue while stimulating ERs in normal tissues.⁵ Tamoxifen (**1**) is a representative antagonist of the ERs in breast tissue and is the most commonly used SERM for the treatment of breast cancer (Figure 1). However, despite the fact that many patients benefit from tamoxifen, resistance to it often emerges, resulting in therapeutic failure.^{6,7} Aromatase inhibitors (AIs), which prevent the formation of estradiol, were developed for the treatment of ER-positive breast cancer during the 1980's.⁸ They have shown superior clinical efficacy compared to tamoxifen in postmenopausal breast cancer patients,⁸ and are considered as an alternative strategy for tamoxifen-resistant breast cancer. Unfortunately, the use of AIs is accompanied with significant side effects, including reduction of bone density, severe musculoskeletal pain, and increased frequency of fractures and cardiovascular events.⁹⁻¹²

Combination endocrine therapy has emerged as an effective cancer treatment paradigm.¹³ Several clinical trials have revealed a significant benefit resulting from combination endocrine therapy involving administration of a SERM and an AI.^{14,15} However, this approach has some

drawbacks. For example, in the ATAC trial, the combination of anastrozole (an AI) and tamoxifen (a SERM) was less effective than anastrozole alone.¹⁶ Moreover, a patient who takes a number of different drugs is at greater risk for side effects and drug interactions.

Dual AI/SERMs might be expected to be more effective than the conventional combination of tamoxifen and an AI. The ER blocking activity of a dual AI/SERM in cancer cells might act synergistically with the AI activity to inhibit cancer cell proliferation, while in normal tissues the ER stimulation of a dual AI/SERM would be expected to alleviate the side effects resulting from the global estrogen depletion caused by the AI activity of the dual AI/SERM. This therapeutic hypothesis motivated the search for compounds that inhibit aromatase and bind to estrogen receptors. Norendoxifen (**4**, Figure 1) was found to be an active tamoxifen metabolite that binds to ERs and is also a potent AI,^{17, 18} and that discovery has provided a platform for the design and synthesis of dual AI/SERMs based on the structure of norendoxifen.¹⁸⁻²⁰ Subsequent work proved that installation of a 4'-hydroxy group on norendoxifen to make the metabolite **5** increased potency vs. aromatase and the two estrogen receptors.¹⁹ More recently, it was determined that the aminoethoxy side chain of norendoxifen can be replaced by a phenolic hydroxyl group and the activity vs. all three receptors (AI, ER- α , and ER- β) maintained as long as the ethyl group is replaced by an imidazolylmethyl moiety (e.g. compound **6**) that can coordinate to the iron of aromatases.²⁰ Initial attempts to install a 4'-amino group in norendoxifen derivatives led to mixed results that were generally disappointing with regard to simultaneous binding to all three receptors.²⁰ In spite of that, the present investigation was launched in an attempt to simultaneously optimize activity against aromatase, ER- α , and

ER- β by replacement of the hydroxyl groups of 4'-hydroxynorendoxifen (**5**) derivatives with amino groups or nitro groups and elimination of the 2'-aminoethyl moiety. The hypothesis was that activity against aromatase, ER- α , and ER- β could be maintained in aminated derivatives even in the absence of imidazole and aminoethyl functionality using a structure-based drug design approach that would take advantage of the known structures of the receptors.

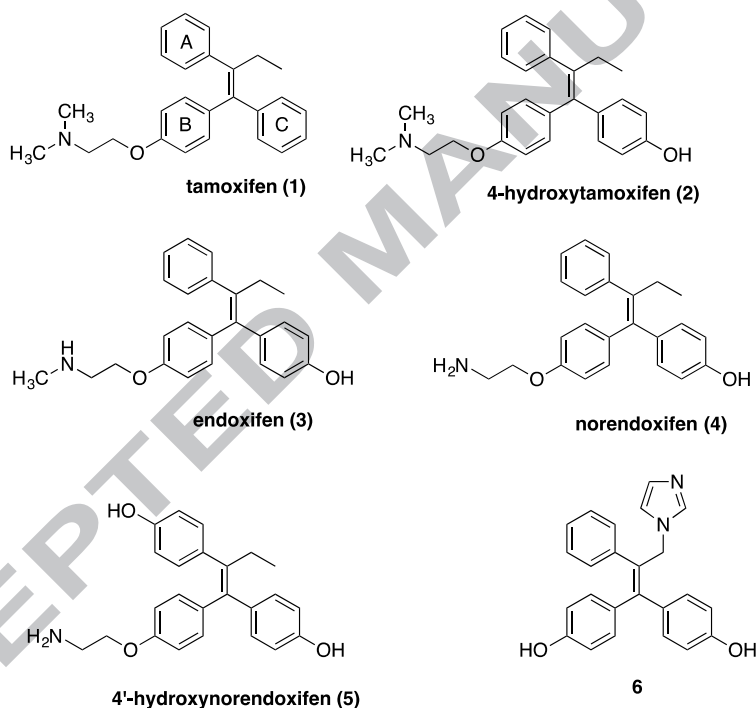


Figure 1. Structures of the SERM tamoxifen (**1**) and its metabolites 4-hydroxytamoxifen (**2**), endoxifen (**3**), norendoxifen (**4**), and 4'-hydroxynorendoxifen (**5**), and an active synthetic imidazole analogue **6**.

Of the third generation AIs, letrozole is 2-5 fold more potent than anastrozole and exemestane in its inhibition of aromatase in noncellular systems and 10-20 fold more potent in cellular systems (Figure 2).²¹ The structure of letrozole consists of two pharmacophores. One is the triazole ring. The other is the symmetrically substituted diphenylmethane fragment that has two identical substituents incorporated at the 4- and 4'-positions. The incorporation of a basic nitrogen and a symmetrically substituted diphenylmethane fragment into norendoxifen analogues might therefore provide an approach to optimize aromatase inhibition (Figure 3). Therefore, norendoxifen was modified by the removal of the aminoethoxyl side chain and introduction of a nitro or amino group in the para position of the "A" ring (Figure 3). The resulting compounds have no geometrical isomers and, similar to anastrozole and letrozole, they also incorporate hydrogen bond acceptors.

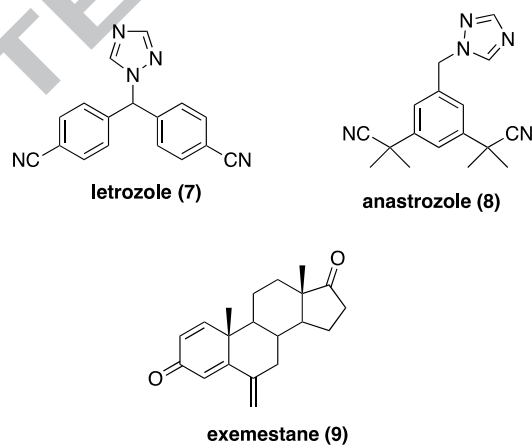


Figure 2. Structures of the third generation AIs letrozole (7), anastrozole (8) and exemestane (9).

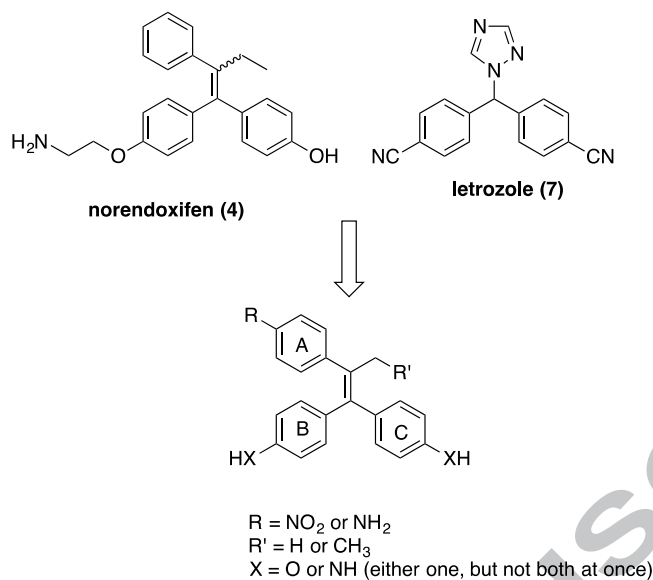
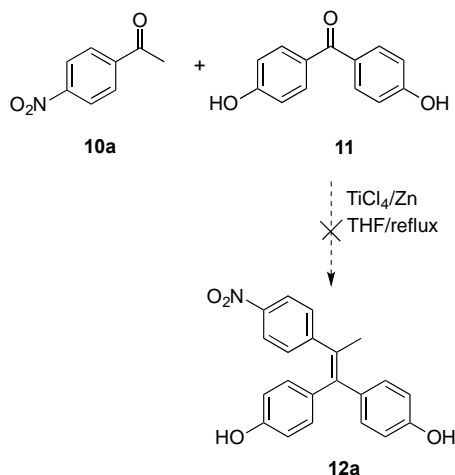


Figure 3. Design strategy for hybrid AI/SERMs.

3. Results and Discussion

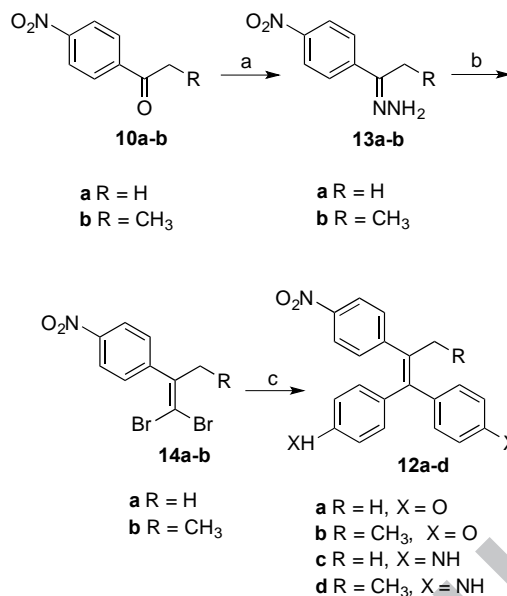
3.1 Synthesis and Evaluation of Triphenylethylenes 12a-d.

The importance of the nitro group as an H-bond acceptor in potent and selective AIs has been emphasized previously by Gobbi and co-workers.²² Initial attempts were made to synthesize the desired nitrated triphenylethylenes **12** by McMurry coupling of benzophenones with propiophenones using the methodology previously reported by our group and others.²³⁻²⁵ However, when 4-nitroacetophenone **10a** was treated with 4,4'-dihydroxybenzophenone **11** in dry THF in the presence of TiCl₄ and Zn, none of the desired McMurry product **12a** was observed (Scheme 1). Attempts to use BOC-protected 4-aminoacetophenone in place of 4-nitroacetophenone **10a** were uniformly unsuccessful.



Scheme 1. Attempted Preparation of 12a through the McMurry Reaction.

The failure of the McMurry approach led to another strategy to transform **10a** into **12a**, namely conversion of ketone **10a** into a 1,1-dibromo-1-alkene **14a** before performing palladium-catalyzed coupling reactions.^{26, 27} Subsequent coupling of **14a** with 4-hydroxyphenylboronic acid under Suzuki conditions proceeded smoothly to provide the desired product **12a** in good yield (67%) (Scheme 2).

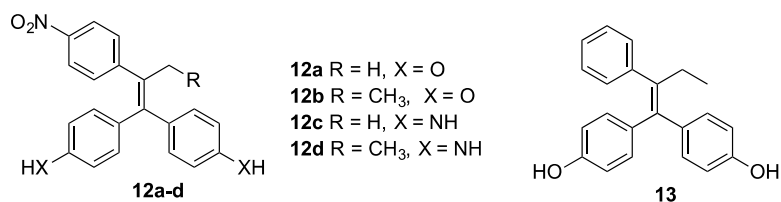


Scheme 2. Synthesis of **12a-d**. Reagents and conditions: (a) $\text{N}_2\text{H}_4 \cdot \text{H}_2\text{O}$, EtOH; (b) CBr_4 , CuCl, DMSO; (c) 4-(HO)PhB(OH)₂ or 4-(H₂N)PhB(OH)₂, $\text{PdCl}_2(\text{PPh}_3)_2$, Na_2CO_3 , THF-H₂O.

The analogues **12b-d** were prepared by employing the same strategy as that used for the synthesis of compound **12a** (Scheme 2). The nitro-substituted ketones **10a** and **10b** were initially treated with hydrazine hydrate at reflux in EtOH to provide the hydrazones **13a** and **13b** in 85% and 90% yields, respectively.²⁶ The hydrazones **13a** and **13b** were reacted with CBr_4 in the presence of CuCl to provide the 1,1-dibromo-1-alkenes **14a** and **14b** in 65% and 50% yields, respectively.²⁷ Finally, the bis-Suzuki arylation of **14a** and **14b** with 4-hydroxyphenylboronic acid or 4-aminophenylboronic acid in the presence of $\text{PdCl}_2(\text{PPh}_3)_2$ at 70 °C in THF-H₂O resulted in the formation of **12a-d** in 47-57% yields.

Compounds **12a-d** were evaluated for their aromatase inhibitory activities and ER binding affinities (Table 1). The IC₅₀ and EC₅₀ values for the previously reported compounds **13**,

(*E,Z*)-norendoxifen, (*E*)-norendoxifen, and (*Z*)-norendoxifen are included for comparison.¹⁸ The results indicate that nitro-substituted bis-phenol compounds **12a** and **12b** are very weak AIs with 75% and 78% inhibition at 50 μ M, respectively. However, the aniline-type compounds **12c** and **12d** exhibited remarkably improved inhibitory activity against aromatase and affinity for ER- α and ER- β when compared with the unsubstituted derivative **13** and with the phenols **12a** and **12b**. They were 113 and 400 times more potent than **13** against aromatase (IC_{50} 220.8 and 62.2 vs 24880 nM), respectively. Compound **12d** showed slightly improved aromatase inhibitory activity and slightly decreased binding affinity to both ER- α and ER- β when compared with the lead compound (*E,Z*-norendoxifen). These results indicate that the replacement of the two phenols of **13** with amino groups and the introduction of a *p*-nitro group in the A-ring contribute in a positive way to both aromatase inhibition and ER binding affinity. Another conclusion that can be drawn is that the aminoethoxyl side chain is important for the hydroxyl-substituted norendoxifen analogues to retain optimal ER binding affinity and aromatase inhibitory activity, but it is not an essential requirement for amino-substituted analogues.

Table 1Aromatase inhibitory activities and ER binding affinities of **12a-d**^{a,b,c}

compd	aromatase (IC ₅₀ , nM, or percent inhibition)	ER-α (EC ₅₀ , nM, or percent competition)	ER-β (EC ₅₀ , nM, or percent competition)
12a	75% inhibition at 50 μM	19% competition at 100 μM	55% competition at 100 μM
12b	78% inhibition at 50 μM	40% competition at 100 μM	66% competition at 100 μM
12c	220.8 ± 42.2	212.9 ± 53.7	486.2 ± 239.5
12d	62.2 ± 7.8	72.1 ± 42.6	70.8 ± 5.2
13	24880 ± 7.8	80% competition at 100 μM	306.9 ± 106.4
(E,Z)-norendoxifen	102.2 ± 32.7	26.9 ± 4.8	35.2 ± 16.8
(E)-norendoxifen	76.8 ± 33.3	58.7 ± 1.0	78.5 ± 57.3
(Z)-norendoxifen	1029 ± 318	17.0 ± 1.9	27.5 ± 14.3
Estradiol		5.7	5.6

^aIC₅₀ values were determined for compounds exhibiting inhibition values higher than 90%.^bPercent aromatase inhibition was determined at the concentration of 50000 nM for each compound.^cPercent ER competition was determined at the concentration of 100000 nM for each compound.

Molecular modeling was performed in order to investigate the binding mode of **12d** in the active sites of aromatase and ER- α . The dianiline **12d** was docked in the active sites of aromatase (PDB code 3s79²⁸) and ER- α (PDB code 3ert²⁹) using GOLD 3.0. These studies capitalized on the secure molecular modeling foundation established by previous investigations of the binding of (*E*)-norendoxifen and several analogues to both aromatase and ER- α , which involved GOLD 3.0 docking, Amber 10 molecular dynamics simulations and Amber parm99 energy minimizations, as well as MM-PBSA binding energy calculations¹⁸⁻²⁰. The calculated models were consistent with experimentally determined SAR. As shown in Figure 4, the overall pose of the ligand is close to that present in the previously published models of (*E*)-norendoxifen and its analogues bound to aromatase.¹⁸⁻²⁰ The amino group on the aniline ring that is trans to the nitrophenyl ring hydrogen bonds to the backbone carbonyl of Asp309. In common with the present situation, all of the previously published models involve hydrogen bonding to Asp309. However, the present model is different in that the amino group on the aniline ring that is cis to the nitrophenyl does not hydrogen bond to backbone carbonyl of Leu372. This may be related to the fact that all of the previously modeled compounds were phenols instead of anilines.

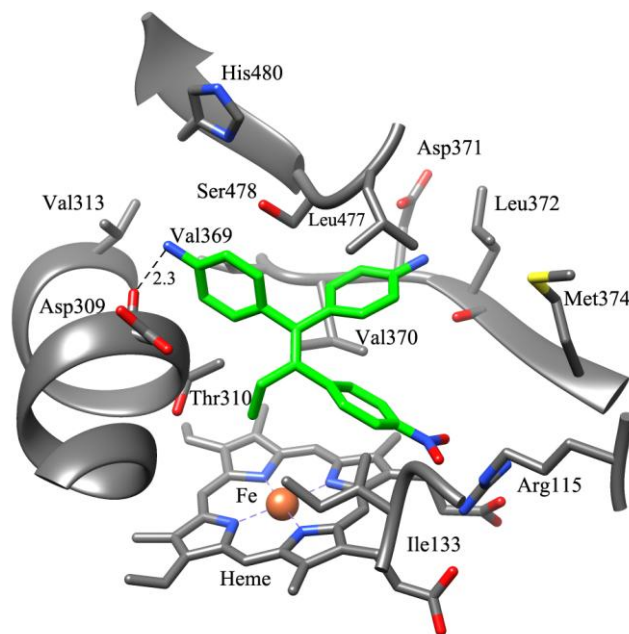


Figure 4. Hypothetical molecular model of **12d** bound in the active site of aromatase (PDB code 3s79²⁸).

The molecular model calculated for the binding of **12d** to ER- α is displayed in Figure 5. In this case, the amino group on the phenyl ring that is cis to the nitrophenyl ring hydrogen bonds to the hydroxyl of Thr347 while the other amino group hydrogen bonds to the carboxylate of Glu353 and the backbone carbonyl of Phe404. The overall pose and the involvement of Thr347 and Glu353 are similar to that in the previously published model of (*Z*)-norendoxifen and one of its analogues bound to ER- α .²⁰ On the other hand, the present case differs in the hydrogen bonding to Phe404 instead of Arg394.²⁰

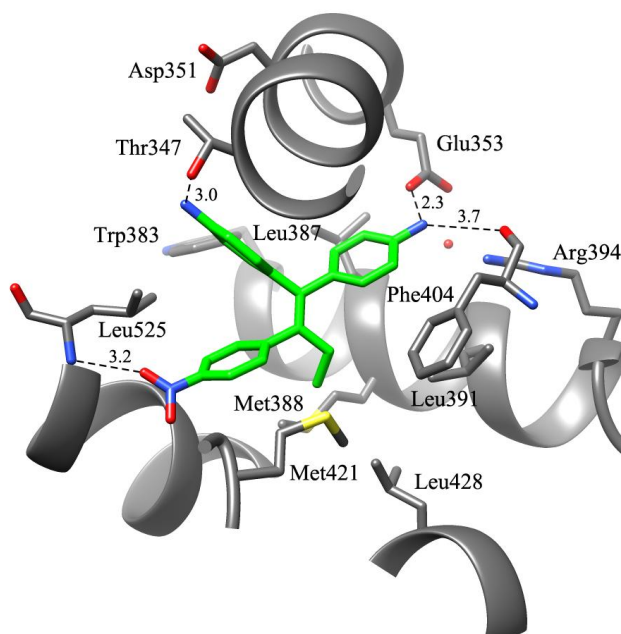
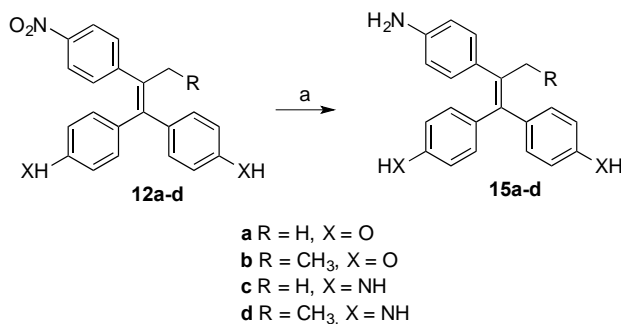


Figure 5. Hypothetical molecular model of **12d** bound in the active site of ER- α (PDB code 3ert²⁹).

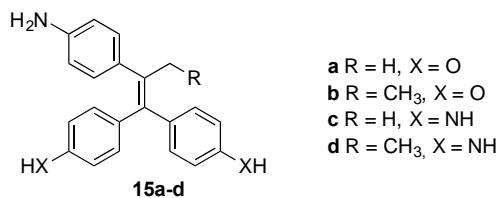
3.2 Synthesis and Evaluation of Triphenylethylenes **15a-d**

The encouraging findings for **12c** and **12d** reported in Table 1 led to the preparation of compounds **15a-d** to explore the effect of replacing the "A" ring nitro group with an amino group as shown in Scheme 3. Compounds **15a-d** were easily obtained in 52-80% yield by reduction of the corresponding nitrosubstituted triphenylalkenes **12a-d** with SnCl₂ (Scheme 3).



Scheme 3. Synthesis of **15a-d**. Reagents and conditions: (a) SnCl₂, EtOH.

The biological results for compounds **15a-d** are summarized in Table 2. Replacement of the nitro groups in **12a-d** with amino groups produced mixed results on the binding affinity with the ERs while all four amino compounds showed significantly improved inhibitory activity against aromatase. In particular, compound **15b** was the most potent of the AIs synthesized in this project with an IC_{50} value of 8.8 nM, which is close to the widely prescribed AI letrozole ($IC_{50}=5.3$ nM³⁰). These results clearly demonstrate the important role played by the "A" ring amino group in **15b** and **15d** in increasing the aromatase inhibitory activity compared to norendoxifen, the nitro derivatives **12b** and **12d**, and unsubstituted compound **13**.

Table 2Aromatase inhibitory activities and ER binding affinities of **15a-d**^{a,b}

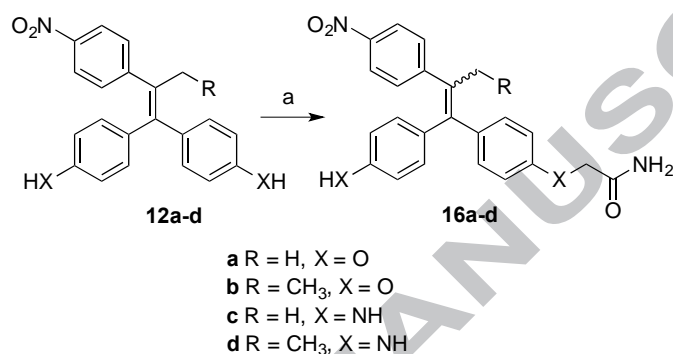
compd	aromatase (IC ₅₀ , nM)	ER- α (EC ₅₀ , nM, or percent competition)	ER- β (EC ₅₀ , nM, or percent competition)
15a	230.0 \pm 11.4	11036 \pm 827	857 \pm 389
15b	8.8 \pm 1.6	1711 \pm 630	1263 \pm 424
15c	177.1 \pm 20.2	31% competition at 100 μ M	77% competition at 100 μ M
15d	13.4 \pm 3.0	25% competition at 100 μ M	76% competition at 100 μ M
Estradiol		5.7	5.6

^aIC₅₀ values were determined for compounds exhibiting inhibition values higher than 90%.^bPercent ER competition was determined at the concentration of 100000 nM for each compound.

Comparing **15b** with **15a** reveals a significant increase in potency on aromatase from IC₅₀ 230 to 8.8 nM and from 11036 to 1711 nM in affinity to ER- α . A similar effect on aromatase was observed for compounds **15c** and **15d**. Obviously, the ethyl substituent is better than the methyl when tested on aromatase and ER- α , but it is actually slightly worse vs. ER- β when comparing **15a** to **15b**.

3.3 Synthesis and Evaluation of Triphenylethylenes 16a-d.

Compounds **16a-d** were prepared 30-56% yield by treatment of **12a-d** one equivalent of 2-iodoacetamide in the presence of K_2CO_3 (Scheme 4). This allows comparison of two sets **16a-d** and **12a-d** with respect to ER binding affinity and aromatase inhibition to determine the effect of the amide side chain on the dual interaction.



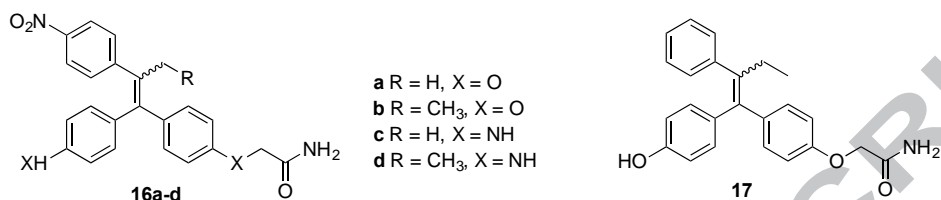
Scheme 4. Synthesis of **16a-d**. Reagents and conditions: (a) ICH_2CONH_2 , acetone, K_2CO_3 ; (b) $LiAlH_4$, $AlCl_3$, THF.

The biological testing results for compounds **16a-d** are summarized in Table 3. IC_{50} and EC_{50} values for the previously reported amide **17** are included for comparison.¹⁸ Substitution of the amino group in one of the phenyl rings of **12c** with the amide side chain in **16c** decreased aromatase inhibitory activity (IC_{50} 220.8 vs 645.3 nM). Compound **16d** also exhibited decreased aromatase inhibitory activity when compared with **12d** (IC_{50} 286.9 vs 62.2 nM). Compounds **16c** and **16d** exhibited elevated potency against both aromatase and ER when compared with **16a**, **16b**, and **17**. The presence of the side chain produced mixed results on the estrogen receptors. It increased affinity when installed on **12c** (compare ER results for **12c** and **16c**), but it decreased

affinity when installed on **12d** (compare ER results for **12d** and **16d**).

Table 3

Aromatase inhibitory activities and ER binding affinities of **16a-d**^{a,b,c}



compd	aromatase (IC ₅₀ , nM, or percent inhibition)	ER-α (EC ₅₀ , nM, or percent competition)	ER-β (EC ₅₀ , nM, or percent competition)
16a	9724 ± 224	0% competition at 100 μM	0% competition at 100 μM
16b	76% inhibition at 50 μM	0% competition at 100 μM	0% competition at 100 μM
16c	645.3 ± 246.4	164.1 ± 96.9	218.4 ± 102.7
16d	286.9 ± 31.8	451.2 ± 201.2	346.4 ± 115.3
17	9257 ± 195	57% competition at 100 μM	71% competition at 100 μM
Estradiol		5.7	5.6

^aIC₅₀ values were determined for compounds exhibiting inhibition values higher than 90%.

^bPercent aromatase inhibition was determined at the concentration of 50000 nM for each

compound. ^cPercent ER competition was determined at the concentration of 100000 nM for each compound.

3.4 Evaluation of Antiestrogenic Effects in a Functional, Cellular Assay.

In order to gain information about the behavior of the triphenylethylenes beyond that

provided by estrogen receptor affinity studies, compounds **12c**, **12d**, **16c**, and **16d** (1 μ M) were tested in a functional assay that measured their abilities to block the effects of β -estradiol (10 nM) in MCF-7 human breast cancer cells. These substances were selected for biological testing because of their relatively high affinity for ER- α and ER- β , and their potencies as estradiol antagonists were compared with endoxifen and (*E,Z*)-norendoxifen. The assay measures progesterone receptor (PGR) mRNA expression level, and the results of the assay are provided in Figure 6. β -Estradiol (10 nM) increased PGR mRNA expression to a level that was assigned the 100% value. Despite the fact that the affinities for ER- α ranged from 451.2 nM (**16d**) to 72.1 nM (**12d**) and those for ER- β ranged from 486.2 nM (**12c**) to 70.8 nM (**12d**), the % RNA expression levels only ranged from 14% (**16c**) to 20% (**12c**) in the functional cellular assay, and the most potent compound in the functional assay (**16c**) was not one with the highest affinity for ER- α and ER- β (**12d** was). Endoxifen, the positive control, was able to antagonize PGR mRNA expression in the presence of 10 nM estradiol (E2) to the level of 3.5%, while the level of expression in the presence of (*E,Z*)-norendoxifen was 22%. These results are generally consistent with those previously reported for structurally related compounds.^{19, 20, 31, 32}

These data indicate that each of the four compounds effectively inhibited the PGR expression. Future dose response studies will be required to determine if there are differences in potencies toward inhibiting the PGR expression or cell proliferation. Since the affinities for the two estrogen receptors varied quite similarly across the compounds, it will be interesting to determine their effects on cell proliferation in light of the studies showing that ER- α and ER- β have opposing effects on breast cancer cells in vitro.³³

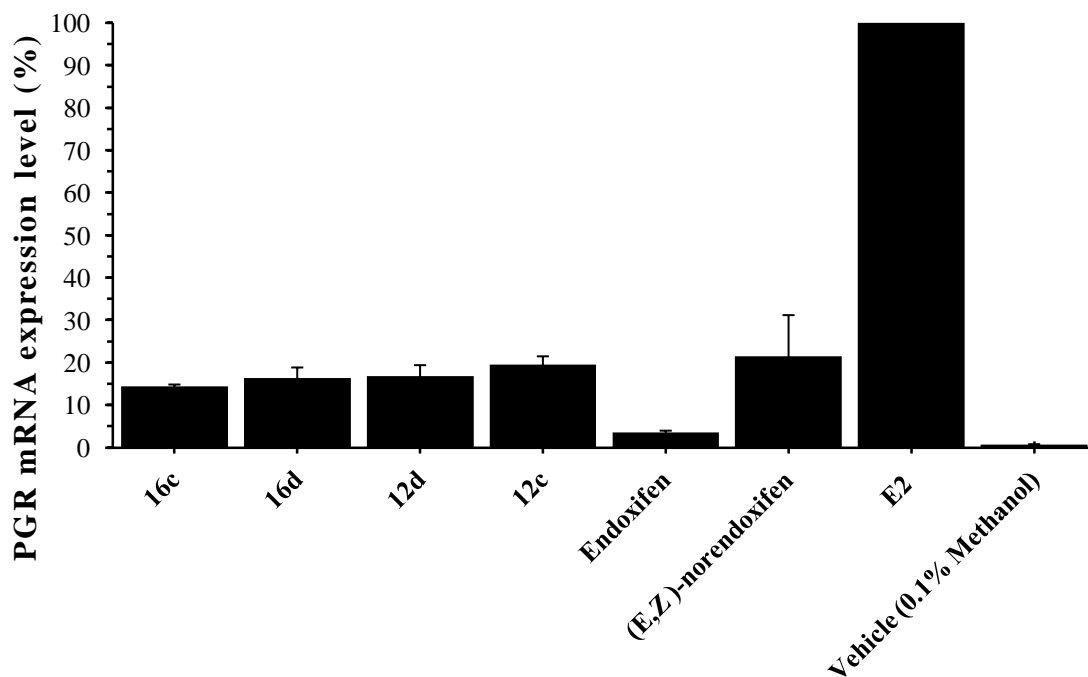
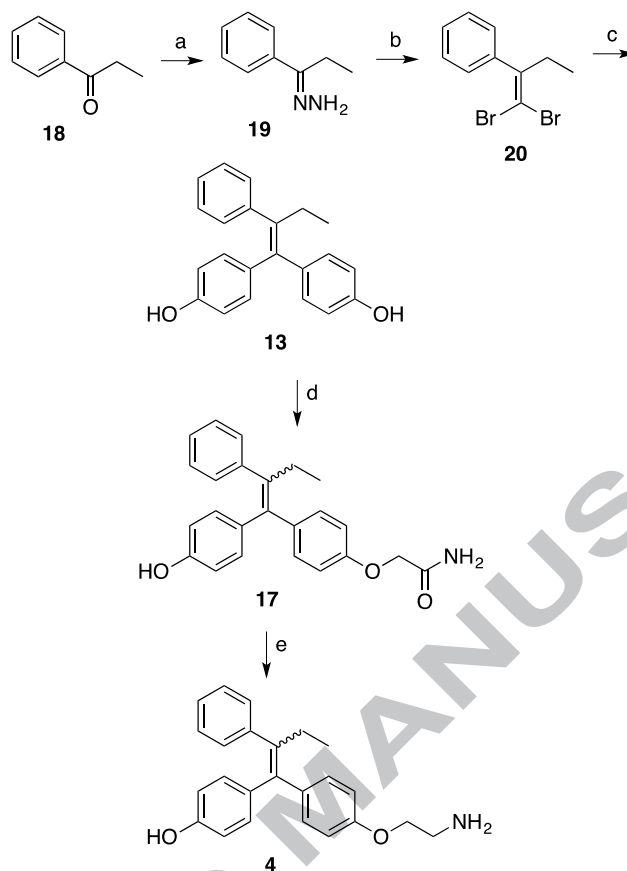


Figure 6. Abilities of compounds **16c**, **16d**, **12d**, **12c**, endoxifen, and (*E,Z*)-norendoxifen (1 μ M) to antagonize β -estradiol (E2, 10 nM)-stimulated progesterone receptor (PGR) mRNA expression in MCF-7 cells. PGR mRNA expression levels relative to estradiol (100%): **16c** (14.1%), **16b** (16.3%), **16c** (16.8%), **16d** (19.6%), endoxifen (3.6%), (*E,Z*)-norendoxifen (21.5%). MCF-7 cells were preconditioned in charcoal-stripped FBS for 72 hours to remove the estrogens. The cells were treated with vehicle (1% methanol), 1 μ M endoxifen or 1 μ M test compound in the presence of 10 nM β -estradiol (E2) and 10 nM β -estradiol alone for 24 hours. Total RNA was isolated from the cells and cDNA was prepared. The E2-stimulated PGR mRNA expression was quantified using a real-time Taqman[®] PCR assay.

3.5 A New Synthesis of (*E,Z*)-Norendoxifen.

Although the first synthesis of (*E,Z*)-norendoxifen through the McMurry reaction was recently reported, the method has limited applicability for the direct synthesis of hydroxylated, nitro, and amino derivatives.¹⁸ A new synthesis of (*E,Z*)-norendoxifen was therefore explored as an extension of the present work (Scheme 5). The synthesis of the triphenylalkene framework commenced with the condensation of propiophenone **18** with hydrazine hydrate in EtOH at reflux to provide the hydrazone **19** in excellent yield (88%).³⁴ 1-(1,1-Dibromobut-1-en-2-yl)benzene **20** was prepared by reaction of hydrazone **19** with CBr₄ (3.0 equiv) in the presence of CuCl (10 mol%) in DMSO in 70% yield.²⁷ The bis-Suzuki arylation of **20** with 4-hydroxyphenylboronic acid in the presence of PdCl₂(PPh₃)₂ (10 mol%) at 70 °C in THF-H₂O resulted in the formation of diphenol **13** in 52% yield. The diphenol **13** was treated with K₂CO₃ and 2-iodoacetamide (1.1 equiv) to afford the amide **21** as the major product in 32% yield. Finally, the reduction of the amide **21** using LiAlH₄ resulted in the generation of (*E,Z*)-norendoxifen in 64% yield.



Scheme 5. Synthesis of (*E,Z*)-Norendoxifen through the Suzuki Coupling Reaction. Reagents and conditions: (a) $\text{N}_2\text{H}_4 \cdot \text{H}_2\text{O}$, EtOH; (b) CBr_4 , CuCl , DMSO; (c) $(\text{HO})_2\text{BPh-4-OH}$, $\text{PdCl}_2(\text{PPh}_3)_2$, Na_2CO_3 , THF- H_2O ; (d) $\text{ICH}_2\text{CONH}_2$, acetone, K_2CO_3 ; (e) LiAlH_4 , AlCl_3 , THF.

4. Conclusion

A series of novel triphenylethylene derivatives based on a symmetrical diphenylmethylene template were designed and synthesized using a new Suzuki bis-arylation approach on an α,α -dibromoalkene. This circumvented problems encountered when the McMurry approach was tried. The para position of the "A" ring of these compounds was substituted with a nitro group or an amino group, while the para position of the "B" and "C" ring

was substituted with a hydroxyl group or an amino group. SAR studies demonstrated that the aminoethoxyl side chain is not an essential requirement for tamoxifen (**1**) analogues to elicit both aromatase inhibitory and ER binding activity despite the fact that many previous reports have argued that it is important for the activity.³⁵⁻³⁹ The introduction of a para-amino group into the A-ring of the triphenylethylene scaffold led to a remarkable improvement of aromatase inhibitory activity (IC_{50} 24880 nM for **13** vs. 8.8 nM for **15b**).

Progress toward the goal to find new classes of AI/SERMs with favorable aromatase inhibitory activity and affinity to ER- α and ER- β was realized with dianiline **12d**, which had potent aromatase inhibitory activity (IC_{50} = 62.2 nM) while also exhibiting high affinity to both ER- α (EC_{50} = 72.1 nM) and ER- β (EC_{50} = 70.8 nM). Moreover, compounds **15b** (IC_{50} = 8.8 nM) and **15d** (IC_{50} = 13.4 nM) displayed highly potent aromatase inhibitory activity that was close to that of the marketed drug letrozole (IC_{50} 5.3 nM) while having low affinity for ER- α and ER- β .

The following conclusions about the structure-activity relationships were drawn: (1) The amino groups in the para positions of the "A" ring and "B" ring play key roles in the modulation of the aromatase inhibitory activity. (2) The unsymmetrical diphenylmethylenesubstructure of norendoxifen can be replaced by a symmetrical diphenylmethylenesubstructure, thereby eliminating E,Z-isomers of the triphenylethylenes and maintaining activity. (3) The replacement of ethyl side chain with a methyl group produced a negative result, whether for aromatase inhibition or ER binding affinity. (4) The aminoethoxyl side chain in triphenylalkene derivatives is not an essential requirement for optimal interaction with the estrogen receptors and aromatase.

Because of their promising biological activities and no complications arising from the

presence of E,Z isomers, the present molecules based on a symmetrical diphenylmethylen template are suitable candidates for further development toward dual AI/SERMs for breast cancer treatment.

ACCEPTED MANUSCRIPT

5. Experimental Section

5.1 Chemistry

Melting points were determined using capillary tubes with a Mel-Temp apparatus and are uncorrected. Reaction products were obtained in pure form directly from reaction mixtures or after column chromatography and did not require additional recrystallization. ^1H NMR and ^{13}C NMR spectra were recorded using a Bruker ARX300 300 MHz spectrometer or a Bruker DPX 400 MHz spectrometer with TMS as internal standard. High-resolution mass spectra (HRMS) were recorded on a double-focusing sector mass spectrometer with magnetic and electrostatic mass analyzers or a Bruker microTOF Q spectrometer. Compound purities were estimated reversed phase C18 by high pressure liquid chromatography (HPLC) with UV detection at 254 nm. The major peak area of each biologically tested compound was $\geq 95\%$ of the combined total peak area. Cytochrome P450 (CYP) inhibitor screening kits for aromatase (CYP19) inhibition studies were purchased from BD Biosciences (San Jose, CA). ER α and β competitor assay kits were purchased from Invitrogen (Carlsbad, CA).

5.1.1 General Procedure for the Synthesis of Hydrazones (13a and 13b).²⁶ A 98% hydrazine monohydrate solution (1 mL, 20 mmol) was added to a suspension of ketone (10 mmol) in EtOH (10 mL). The mixture was heated to reflux for 2 h. After cooling to room temperature, the solid was filtered and the crude hydrazone was washed with H_2O (20 mL X 2) and dried in vacuo. The product was used in the next step without further purification.

5.1.2 1-[1-(4-Nitrophenyl)ethylidene]hydrazine (13a). Brick red solid, 85% yield, mp

149-150 °C (lit.²⁶ mp 148-149 °C).

5.1.3 1-(1-(4-Nitrophenyl)propylidene)hydrazine (13b). Orange crystalline solid, 90% yield, mp 103-104 °C. ¹H NMR (300 MHz, CDCl₃) δ 8.18 (d, *J* = 7.1 Hz, 2 H), 7.80 (d, *J* = 7.1 Hz, 2 H), 5.73 (s, 2 H), 2.64 (q, *J* = 7.7 Hz, 2 H), 1.18 (t, *J* = 7.7 Hz, 3 H); ¹³C NMR (75 MHz, CDCl₃) δ 147.9, 146.2, 144.4, 125.8, 123.6, 17.9, 9.44; CIMS *m/z* 194 (MH⁺); HRCIMS *m/z* calcd for C₉H₁₂N₃O₂ (MH⁺) 194.0924, found 194.0932.

5.1.4 General Procedure for the Synthesis of 1,1-Dibromo-1-alkenes (14a and 14b).²⁷

A 28% aqueous solution of ammonia (1 mL) and CuCl (0.3 mmol) were added to a solution of hydrazones **13a** or **13b** (3.0 mmol) in DMSO (3 mL). Then CBr₄ (9 mmol) in DMSO (5 mL) was added dropwise. The reaction mixture was stirred at room temperature for 16 h and quenched with H₂O (30 mL) and extracted with CH₂Cl₂ (20 mL X 3). After being dried over Na₂SO₄, the CH₂Cl₂ was evaporated and the residue was purified by column chromatography (hexane: EtOAc = 2: 1) to afford the product **14a** or **14b**.

5.1.5 1-(1,1-Dibromoprop-1-en-2-yl)-4-nitrobenzene (14a). White solid, 65% yield, mp 81-82 °C. ¹H NMR (300 MHz, CDCl₃) δ 8.23 (d, *J* = 8.7 Hz, 2 H), 7.41 (d, *J* = 8.7 Hz, 2 H), 2.23 (s, 1 H); ¹³C NMR (75 MHz, CDCl₃) δ 148.5, 141.1, 128.6, 123.8, 123.4, 89.6, 25.9; CIMS *m/z* 321 (MH⁺).

5.1.6 1-(1,1-Dibromobut-1-en-2-yl)-4-nitrobenzene (14b). White solid, 50% yield: mp 57-58 °C. ¹H NMR (300 MHz, CDCl₃) δ 8.24 (d, *J* = 8.7 Hz, 2 H), 7.37 (d, *J* = 8.7 Hz, 2 H), 2.63 (q, *J* = 7.5 Hz, 2 H), 0.98 (t, *J* = 7.4 Hz, 3 H); ¹³C NMR (75 MHz, CDCl₃) δ 147.5, 147.0, 146.9, 129.0, 123.8, 89.3, 32.6, 11.3; CIMS *m/z* 336 (MH⁺); HRCIMS *m/z* calcd for

$C_{10}H_{10}N_1O_2^{79}Br^{81}Br$ (MH^+) 335.9052, found 335.9048.

5.1.7 General Procedure for the Synthesis of Triphenylalkenes (12a-d). A solution of 1,1-dibromo-1-alkenes **14a** or **14b** (1.0 mmol), 4-hydroxyphenylboronic acid or 4-aminophenylboronic acid (4.0 mmol), $PdCl_2(PPh_3)_2$ (0.1 mmol), and Na_2CO_3 (3.0 mmol) in THF- H_2O (15 mL) was heated to 70 °C under Ar_2 for 18 h. After cooling to room temperature, EtOAc (15 mL) and H_2O (10 mL) were poured into the reaction mixture. The aqueous layer was extracted with EtOAc (20 mL X 3). The combined organic layers were washed with water and dried, concentrated in vacuo and purified by flash column chromatography (hexane: EtOAc = 2:1) to afford the products **12a-d**.

5.1.8 4-(1-(4-Hydroxyphenyl)-2-(4-nitrophenyl)prop-1-enyl)phenol (12a). Light brown solid, 67% yield: mp 235-236 °C. 1H NMR (300 MHz, $CDCl_3$) δ 8.02 (d, $J = 9.0$ Hz, 2 H), 7.28 (d, $J = 7.8$ Hz, 2 H), 7.10 (d, $J = 8.1$ Hz, 2 H), 6.82 (d, $J = 8.7$ Hz, 2 H), 6.72 (d, $J = 9.0$ Hz, 2 H), 6.52 (d, $J = 8.4$ Hz, 2 H), 4.78 (s, 1 H), 4.62 (s, 1 H), 2.17 (s, 3 H); ^{13}C NMR (75 MHz, $CDCl_3$) δ 154.7, 154.3, 152.1, 145.5, 141.3, 135.2, 134.9, 132.3, 132.1, 131.3, 130.2, 123.2, 115.0, 114.7, 22.9; ESIMS m/z 370 (MNa^+); HRESIMS m/z calcd for $C_{21}H_{17}NO_4Na$ (MNa^+) 370.1055, found 370.1066; HPLC purity, 100% (90% MeOH, 10% H_2O).

5.1.9 4-(1-(4-Hydroxyphenyl)-2-(4-nitrophenyl)but-1-enyl)phenol (12b). Pale yellow solid, 57% yield: mp 111-112 °C. 1H NMR (300 MHz, methanol- d_4) δ 7.99 (d, $J = 8.7$ Hz, 2 H), 7.29 (d, $J = 8.7$ Hz, 2 H), 7.03 (d, $J = 8.7$ Hz, 2 H), 6.77 (d, $J = 8.1$ Hz, 2 H), 6.66 (d, $J = 8.4$ Hz, 2 H), 6.62 (s, 2 H), 6.44 (d, $J = 9.0$ Hz, 2 H), 2.54 (q, $J = 7.8$ Hz, 2 H), 0.90 (t, $J = 7.8$ Hz, 3 H); ^{13}C NMR (75 MHz, methanol- d_4) δ 157.7, 157.1, 152.3, 147.1, 142.8, 139.6, 135.7, 135.3, 133.3,

132.0, 131.6, 128.5, 124.0, 116.8, 116.5, 115.9, 115.5, 29.5, 14.0; negative ion ESIMS m/z 360 ($M - H^+$)⁻; negative ion HRESIMS m/z calcd for C₂₂H₁₈NO₄ ($M - H^+$)⁻ 360.1236, found 360.1237; HPLC purity, 95.18% (90% MeOH, 10% H₂O).

5.1.10 4-(1-(4-Aminophenyl)-2-(4-nitrophenyl)prop-1-enyl)benzenamine (12c). Brick red solid, 55% yield: mp 202-204 °C. ¹H NMR (300 MHz, methanol-*d*₄) δ 7.97 (d, *J* = 6.6 Hz, 2 H), 7.32 (d, *J* = 7.2 Hz, 2 H), 6.96 (d, *J* = 6.9 Hz, 2 H), 6.71 (d, *J* = 6.9 Hz, 2 H), 6.60 (d, *J* = 6.6 Hz, 2 H), 6.41 (d, *J* = 6.9 Hz, 2 H), 2.16 (s, 3 H); ¹³C NMR (75 MHz, methanol-*d*₄) δ 154.3, 147.4, 146.8, 144.1, 134.4, 133.2, 132.0, 131.8, 131.6, 124.0, 116.2, 115.9, 23.0; ESIMS m/z 346 (MH⁺); HRESIMS m/z calcd for C₂₁H₂₀N₃O₂ (MH⁺) 346.1556, found 346.1572; HPLC purity, 100% (90% MeOH, 10% H₂O).

5.1.11 4-(1-(4-Aminophenyl)-2-(4-nitrophenyl)but-1-enyl)benzenamine (12d). Brick red solid, 40% yield: mp 182-183 °C. ¹H NMR (300 MHz, methanol-*d*₄) δ 7.99 (d, *J* = 8.7 Hz, 2 H), 7.32 (d, *J* = 8.7 Hz, 2 H), 6.95 (d, *J* = 9.0 Hz, 2 H), 6.70 (d, *J* = 8.4 Hz, 2 H), 6.57 (d, *J* = 9.0 Hz, 2 H), 6.38 (d, *J* = 8.4 Hz, 2 H), 2.58 (q, *J* = 7.8 Hz, 2 H), 0.92 (t, *J* = 7.5 Hz, 3 H); ¹³C NMR (75 MHz, methanol-*d*₄) δ 152.9, 147.9, 143.7, 138.6, 134.1, 133.1, 132.1, 131.4, 124.0, 116.1, 115.6, 29.5, 14.0; ESIMS m/z 360 (MH⁺); HRESIMS m/z calcd for C₂₂H₂₂N₃O₂ (MH⁺) 360.1712, found 360.1723; HPLC purity, 97.74% (90% MeOH, 10% H₂O).

5.1.12 General Procedure for the Synthesis of Reduction Products (15a-d). A solution of nitro-containing compounds **12a** or **12b** or **12c** or **12d** (0.3 mmol) and SnCl₂ (1.5 mmol) in ethanol (10 mL) was heated at reflux for 5 h. After the reaction mixture was cooled to room temperature, saturated aq K₂CO₃ solution was slowly added with stirring until the pH was 8-9.

Then the mixture was extracted with EtOAc (10 mL X 3), and the combined organic layer was dried. The solvent was evaporated and the residue was purified by flash column chromatography (EtOAc: hexane = 1:1) to afford the products **15a-d**.

5.1.13 4-(2-(4-Aminophenyl)-1-(4-hydroxyphenyl)prop-1-enyl)phenol (15a). White solid, 80% yield: mp 154-156 °C. ¹H NMR (300 MHz, DMSO-*d*₆) δ 9.34 (s, 1 H), 9.12 (s, 1 H), 6.91 (d, *J* = 8.5 Hz, 2 H), 6.75 (d, *J* = 8.5 Hz, 2 H), 6.70 (d, *J* = 8.5 Hz, 2 H), 6.60 (d, *J* = 8.5 Hz, 2 H), 6.42 (d, *J* = 8.5 Hz, 2 H), 6.32 (d, *J* = 8.5 Hz, 2 H), 4.97 (s, 2 H), 1.95 (s, 3 H); ¹³C NMR (75 MHz, DMSO-*d*₆) δ 156.5, 155.8, 147.4, 137.4, 135.7, 133.7, 132.4, 132.2, 131.7, 130.6, 115.7, 115.2, 114.3, 23.9; MALDIMS *m/z* 317 (M⁺); HRESIMS *m/z* calcd for C₂₁H₂₀NO₂ (MH⁺) 318.1494, found 318.1495; HPLC purity, 97.85% (90% MeOH, 10% H₂O).

5.1.14 4-(2-(4-Aminophenyl)-1-(4-hydroxyphenyl)but-1-enyl)phenol (15b). White solid, 71% yield: mp 173-175 °C. ¹H NMR (300 MHz, DMSO-*d*₆) δ 9.34 (s, 1 H), 9.10 (s, 1 H), 6.93 (d, *J* = 8.5 Hz, 2 H), 6.72 (d, *J* = 8.5 Hz, 2 H), 6.59 (d, *J* = 8.5 Hz, 2 H), 6.40 (d, *J* = 8.5 Hz, 2 H), 6.37 (d, *J* = 8.5 Hz, 2 H), 6.34 (d, *J* = 8.5 Hz, 2 H), 4.92 (s, 2 H), 2.30 (q, *J* = 7.4 Hz, 2 H), 0.84 (t, *J* = 7.4 Hz, 3 H); ¹³C NMR (75 MHz, DMSO-*d*₆) δ 156.7, 155.7, 147.4, 137.7, 135.8, 135.2, 134.9, 132.3, 131.1, 130.8, 115.8, 115.1, 114.5, 29.3, 14.7; MALDIMS *m/z* 331 (M⁺); HRESIMS *m/z* calcd for C₂₂H₂₂NO₂ (MH⁺) 332.1651, found 332.1651; HPLC purity, 99.59% (90% MeOH, 10% H₂O).

5.1.15 4-(1,2-Bis(4-aminophenyl)prop-1-enyl)benzenamine (15c). White solid, 52% yield: mp 134-135 °C. ¹H NMR (300 MHz, DMSO-*d*₆) δ 6.77 (d, *J* = 8.3 Hz, 2 H), 6.75 (d, *J* = 8.3 Hz, 2 H), 6.49 (d, *J* = 8.1 Hz, 2 H), 6.40 (d, *J* = 8.2 Hz, 2 H), 6.32 (d, *J* = 8.4 Hz, 2 H), 6.21

(d, $J = 8.4$ Hz, 2 H), 4.88 (s, 6 H), 1.96 (s, 3 H); ^{13}C NMR (75 MHz, DMSO- d_6) δ 147.7, 147.1, 146.9, 138.4, 132.9, 132.2, 131.6, 131.4, 130.6, 114.3, 113.9, 24.1; MALDIMS m/z 315 (M^+); HRESIMS m/z calcd for $\text{C}_{21}\text{H}_{22}\text{N}_3$ (MH^+) 316.1814, found 316.1814; HPLC purity, 95.50% (90% MeOH, 10% H_2O).

5.1.16 4-(1,2-Bis(4-aminophenyl)but-1-enyl)benzenamine (15d). White solid, 56% yield: mp 145-147 °C. ^1H NMR (300 MHz, DMSO- d_6) δ 6.77 (d, $J = 8.3$ Hz, 2 H), 6.73 (d, $J = 8.3$ Hz, 2 H), 6.49 (d, $J = 8.3$ Hz, 2 H), 6.45 (d, $J = 8.4$ Hz, 2 H), 6.34 (d, $J = 8.3$ Hz, 2 H), 6.20 (d, $J = 8.4$ Hz, 2 H), 4.89 (s, 6 H), 2.33 (q, $J = 7.4$ Hz, 2 H), 0.83 (t, $J = 7.2$ Hz, 3 H); ^{13}C NMR (75 MHz, DMSO- d_6) δ 147.7, 147.1, 146.7, 138.6, 133.1, 132.8, 132.1, 131.0, 130.8, 130.7, 129.8, 129.1, 114.5, 114.4, 113.9, 29.2, 14.8; MALDIMS m/z 329 (M^+); HRESIMS m/z calcd for $\text{C}_{22}\text{H}_{24}\text{N}_3$ (MH^+) 330.1970, found 330.1971; HPLC purity, 96.91% (90% MeOH, 10% H_2O).

5.1.17 General Procedure for the Synthesis of the Monoalkylated Products (16a-d).

A suspension of the diphenols **12a** or **12b** or dianilines **12c** or **12d** (1 mmol) and K_2CO_3 (3 mmol) in acetone (10 mL) was heated at reflux for 10 min. A solution of 2-iodoacetamide (1.3 mmol) in acetone (6 mL) was added in small portions over 3 h and the reaction mixture was heated at reflux for an additional 1 h. After cooling to room temperature, the solvent was evaporated and the residue was dissolved in saturated NH_4Cl solution (30 mL) and extracted with EtOAc (30 mL X 3). The organic layers were combined, dried, concentrated in vacuo and purified by flash column chromatography to provide the products **16a-d**.

5.1.18

(*E,Z*)-2-(4-(1-(4-Hydroxyphenyl)-2-(4-nitrophenyl)prop-1-enyl)phenoxy)-acetamide (16a).

Yellow solid, 41% yield: mp 129-130 °C. ^1H NMR (300 MHz, methanol- d_4) δ 7.99 (d, $J = 9.3$ Hz, 2 H, isomer 1), 7.98 (d, $J = 8.7$ Hz, 2 H, isomer 2), 7.34 (d, $J = 9.3$ Hz, 2 H, isomer 1), 7.33 (d, $J = 8.7$ Hz, 2 H, isomer 2), 7.17 (d, $J = 8.7$ Hz, 2 H, isomer 2), 7.02 (d, $J = 8.4$ Hz, 2 H, isomer 1), 6.98 (d, $J = 8.0$ Hz, 2 H, isomer 1), 6.82-6.76 (m, 4 H), 6.66 (d, $J = 8.7$ Hz, 4 H), 6.46 (d, $J = 8.7$ Hz, 2 H, isomer 2), 4.51 (s, 2 H, isomer 1), 4.53 (s, 2 H, isomer 2), 2.15 (s, 3 H, isomer 1), 2.13 (s, 3 H, isomer 2); ^{13}C NMR (75 MHz, methanol- d_4) δ 174.0, 174.0, 158.2, 157.8, 157.7, 157.4, 153.5, 147.1, 142.8, 137.9, 137.7, 135.2, 135.0, 133.8, 133.6, 133.3, 133.3, 133.1, 132.3, 132.2, 131.6, 124.1, 116.0, 115.6, 115.5, 115.0, 67.9, 67.8, 23.2, 23.0; negative ion ESIMS m/z 403 ($\text{M} - \text{H}^+$) $^-$; HRESIMS m/z calcd for $\text{C}_{23}\text{H}_{21}\text{N}_2\text{O}_5$ (MH^+) 405.1450, found 405.1460; HPLC purity, 95.55% (90% MeOH, 10% H_2O).

5.1.19

(*E,Z*)-2-(4-(1-(4-Hydroxyphenyl)-2-(4-nitrophenyl)but-1-enyl)phenoxy)-acetamide (16b).

Yellow oil, 56% yield. ^1H NMR (300 MHz, methanol- d_4) δ 8.01 (d, $J = 8.7$ Hz, 2 H, isomer 1), 8.00 (d, $J = 8.7$ Hz, 2 H, isomer 2), 7.32 (d, $J = 8.7$ Hz, 2 H, isomer 1), 7.31 (d, $J = 8.7$ Hz, 2 H, isomer 2), 7.15 (d, $J = 8.7$ Hz, 2 H, isomer 2), 7.00 (d, $J = 8.4$ Hz, 2 H, isomer 1), 6.97 (d, $J = 8.0$ Hz, 2 H, isomer 1), 6.79-6.76 (m, 4 H), 6.64 (d, $J = 8.7$ Hz, 4 H), 6.44 (d, $J = 8.7$ Hz, 2 H, isomer 2), 4.51 (s, 2 H, isomer 1), 4.34 (s, 2 H, isomer 2), 2.59-2.50 (m, 4 H), 0.94-0.89 (m, 6 H); ^{13}C NMR (75 MHz, methanol- d_4) δ 174.1, 158.2, 157.8, 157.2, 152.0, 147.2, 142.2, 140.5, 140.2, 137.9, 137.6, 135.3, 135.0, 133.3, 133.2, 132.1, 131.7, 131.6, 124.1, 116.0, 115.6, 115.0, 68.0, 67.8, 29.6, 29.5, 13.9; ESIMS m/z 441 (MNa^+); HRESIMS m/z calcd for $\text{C}_{24}\text{H}_{22}\text{N}_2\text{O}_5\text{Na}$ (MNa^+) 441.1427, found 441.1431; HPLC purity, 97.18% (90% MeOH, 10% H_2O).

5.1.20**(*E,Z*)-2-(4-(1-(4-Aminophenyl)-2-(4-nitrophenyl)prop-1-enyl)phenylamino)acetamide (16c).**

Reddish-brown solid, 30% yield: mp 112-114 °C. ¹H NMR (300 MHz, methanol-*d*₄) δ 7.98 (d, *J* = 8.8 Hz, 2 H, isomer 1), 7.97 (d, *J* = 8.8 Hz, 2 H, isomer 2), 7.33 (d, *J* = 8.7 Hz, 2 H, isomer 1), 7.32 (d, *J* = 8.7 Hz, 2 H, isomer 2), 6.97 (d, *J* = 8.4 Hz, 2 H, isomer 1), 6.95 (d, *J* = 8.4 Hz, 2 H, isomer 2), 6.70 (d, *J* = 8.5 Hz, 2 H, isomer 1), 6.65-6.58 (m, 6 H), 6.41 (d, *J* = 8.5 Hz, 2 H), 6.28 (d, *J* = 8.5 Hz, 2 H), 3.94 (s, 2 H, isomer 1), 3.75 (s, 2 H, isomer 2), 2.15 (s, 6 H); ¹³C NMR (75 MHz, methanol-*d*₄) δ 177.1, 154.3, 148.3, 148.0, 146.8, 134.7, 133.9, 133.2, 132.1, 132.0, 131.7, 124.0, 116.1, 115.9, 113.3, 112.9, 23.1; ESIMS *m/z* 425 (MNa⁺); HRESIMS *m/z* calcd for C₂₃H₂₃N₄O₃ (MH⁺) 403.1770, found 403.1776; HPLC purity, 97.57% (90% MeOH, 10% H₂O).

5.1.21**(*E,Z*)-2-(4-(1-(4-Aminophenyl)-2-(4-nitrophenyl)but-1-enyl)phenylamino)acetamide (16d).**

Reddish-brown solid, 34% yield: mp 132-135 °C. ¹H NMR (300 MHz, methanol-*d*₄) δ 7.99 (d, *J* = 8.8 Hz, 2 H, isomer 1), 7.98 (d, *J* = 8.8 Hz, 2 H, isomer 2), 7.32 (d, *J* = 8.7 Hz, 2 H, isomer 1), 7.30 (d, *J* = 8.7 Hz, 2 H, isomer 2), 7.01 (d, *J* = 8.4 Hz, 2 H, isomer 1), 7.00 (d, *J* = 8.4 Hz, 2 H, isomer 2), 6.82 (d, *J* = 8.5 Hz, 2 H, isomer 1), 6.68-6.58 (m, 6 H), 6.50 (d, *J* = 8.5 Hz, 2 H), 6.26 (d, *J* = 8.5 Hz, 2 H), 3.75 (s, 2 H, isomer 1), 3.60 (s, 2 H, isomer 2), 2.61-2.52 (m, 4 H), 0.95-0.88 (m, 6 H); ¹³C NMR (75 MHz, methanol-*d*₄) δ 177.1, 152.5, 148.6, 148.0, 147.0, 143.1, 139.3, 136.3, 133.7, 133.2, 133.1, 132.1, 131.5, 124.1, 117.4, 117.2, 113.4, 112.9, 29.6, 14.0; ESIMS *m/z* 417 (MH⁺); HRESIMS *m/z* calcd for C₂₄H₂₅N₄O₃ (MH⁺) 417.1927, found 417.1935; HPLC purity, 96.48% (90% MeOH, 10% H₂O).

5.1.22 1-(1-Phenylpropylidene)hydrazine (19).³⁴ A 98% hydrazine monohydrate solution (2 mL, 40 mmol) was added to propiophenone (**18**, 2.68 g, 20 mmol) in EtOH (15 mL). The mixture was heated to reflux for 2 h. After cooling to room temperature, the mixture was partitioned between CH₂Cl₂ and H₂O. The aqueous layer was extracted with CH₂Cl₂ (30 mL X 3). The organic layers were combined, dried, concentrated in vacuo and purified by column chromatography (hexane: EtOAc = 5: 1) to afford the product **19** as yellowish solid (2.60 g, 88% yield): mp 52-53 °C (lit.³⁴ mp 55-57 °C).

5.1.23 1-(1,1-Dibromobut-1-en-2-yl)benzene (20).²⁷ A 28% aqueous solution of ammonia (1 mL) and CuCl (29.7 mg, 0.3 mmol) were added to a solution of 1-(1-phenylpropylidene)hydrazine **19** (444 mg, 3.0 mmol) in DMSO (3 mL). Then CBr₄ (2.98 g, 9 mmol) in DMSO (5 mL) was added dropwise. The reaction mixture was stirred at room temperature for 16 h and quenched with H₂O (30 mL) and extracted with CH₂Cl₂ (20 mL X 3). After being dried over Na₂SO₄, the CH₂Cl₂ was evaporated and the residue was purified by column chromatography (hexane) to afford the product **12** as a light brown oil (607 mg, 70% yield). ¹H NMR (400 MHz, CDCl₃) δ 7.39-7.30 (m, 3 H), 7.19-7.16 (m, 2 H), 2.61 (q, *J* = 7.6 Hz, 2 H), 0.98 (t, *J* = 7.6 Hz, 3 H); ¹³C NMR (100 MHz, CDCl₃) δ 148.9, 140.9, 128.4, 127.9, 127.7, 87.5, 32.8, 11.4; CIMS *m/z* 290 (MH⁺).

5.1.24 4-(1-(4-Hydroxyphenyl)-2-phenylbut-1-enyl)phenol (13). A solution of 1-(1,1-dibromobut-1-en-2-yl)benzene **20** (288 mg, 1.0 mmol), 4-hydroxyphenylboronic acid (552 mg, 4.0 mmol), PdCl₂(PPh₃)₂ (70 mg, 0.1 mmol), and Na₂CO₃ (318 mg, 3.0 mmol) in THF-H₂O (4:1, 15 mL) was heated to 70 °C under Ar₂ for 18 h. After cooling to room

temperature, EtOAc (15 mL) and H₂O (10 mL) were poured into the reaction mixture. The aqueous layer was extracted with EtOAc (20 mL X 3). The combined organic layers were washed with water and dried, concentrated in vacuo and purified by silica gel flash column chromatography (hexane: EtOAc = 4:1) to afford the product **13** as white solid (164 mg, 52% yield): mp 198-200 °C. ¹H NMR (400 MHz, DMSO-*d*₆) δ 9.40 (s, 1 H), 9.15 (s, 1 H), 7.18 (t, *J* = 7.6 Hz, 2 H), 7.10 (t, *J* = 7.6 Hz, 3 H), 6.98 (d, *J* = 8.8 Hz, 2 H), 6.75 (d, *J* = 8.4 Hz, 2 H), 6.60 (d, *J* = 8.4 Hz, 2 H), 6.40 (d, *J* = 8.8 Hz, 2 H), 2.41 (q, *J* = 7.2 Hz, 2 H), 0.84 (t, *J* = 7.2 Hz, 3 H); ¹³C NMR (100 MHz, DMSO-*d*₆) δ 156.8, 155.9, 143.2, 140.1, 139.0, 134.8, 134.6, 132.2, 130.9, 130.2, 128.6, 126.6, 115.7, 115.0, 29.3, 14.2; HRAPCIMS *m/z* calcd for C₂₂H₂₁O₂ (MH⁺) 317.1542, found 317.1565.

5.1.25 (*E,Z*)-2-(4-(1-(4-Hydroxyphenyl)-2-phenylbut-1-enyl)phenoxy)-acetamide (17).

The intermediate was prepared as previously described.¹⁸

5.1.26 (*E,Z*)-Norendoxifen. This compound was prepared as previously described.¹⁸

5.2 Inhibition of Recombinant Human Aromatase (CYP19) by Microsomal Incubations. These experiments were conducted as previously described.¹⁹

5.3 Binding Affinities for Recombinant Human ER- α and ER- β . The binding affinities were determined as previously described.¹⁹

5.4 Abilities of Compounds to Antagonize β -Estradiol-stimulated Progesterone Receptor (PGR) mRNA Expression in MCF-7 Cells. The assay was performed as previously described.¹⁹

Corresponding Author

Mark Cushman, Pharm.D., Ph.D.

Department of Medicinal Chemistry and Molecular Pharmacology, College of Pharmacy, and
The Purdue University Center for Cancer Research, Purdue University, 575 Stadium Mall Drive,
West Lafayette, Indiana 47907, United States

Tel: 765-494-1465

Fax: 765-494-6790

e-mail: cushman@purdue.edu

Acknowledgments

This research was supported by the Purdue University Center for Cancer Research and the Indiana University Center Joint Funding Award 206330, and by the Purdue Center for Cancer Research grant P30 CA023168.

Abbreviations

AIs, aromatase inhibitors; ATAC, arimidex, tamoxifen, alone or in combination; DMSO, dimethyl sulphoxide; ER, estrogen receptor; EtOAc, ethyl acetate; EtOH, ethanol; MeOH, methanol; SAR, structure-activity relationship; SERM, selective estrogen receptor modulator; THF, tetrahydrofuran.

Supplementary data

SMILES molecular strings and PDB files for **12d** bound to aromatase and ER- α , as well as ^1H and ^{13}C NMR spectra for compounds **12-16** and **20**.

Keywords

Aromatase inhibitor

Estrogen receptor

Breast cancer

Antiestrogenic activity

(*E,Z*)-Norendoxifen synthesis

References

1. Amir, E.; Freedman, O. C.; Seruga, B.; Evans, D. G. *J. Natl. Cancer Inst.* **2010**, *102*, 680.
2. Bai, Z.; Gust, R. *Arch. Pharm.* **2009**, *342*, 133.
3. Ali, S.; Coombes, R. C. *J. Mammary Gland Biol. Neoplasia* **2000**, *5*, 271.
4. Jordan, V. C.; McDaniel, R.; Agboke, F.; Maximov, P. Y. *Steroids* **2014**, *90*, 3.
5. Komm, B. S.; Mirkin, S. *J. Steroid Biochem. Mol. Biol.* **2014**, *143*, 207.
6. Ring, A.; Dowsett, M. *Endocr. Relat. Cancer* **2004**, *11*, 643.
7. Ali, S.; Coombes, R. C. *Nat. Rev. Cancer* **2002**, *2*, 101.
8. Chumsri, S.; Howes, T.; Bao, T.; Sabnis, G.; Brodie, A. *J. Steroid Biochem. Mol. Biol.* **2011**, *125*, 13.
9. Heshmati, H. M.; Khosla, S.; Robins, S. P.; O'Fallon, W. M.; Melton, L. J.; Riggs, B. L. *J. Bone Miner. Res.* **2002**, *17*, 172.
10. Bundred, N. J. *Br. J. Cancer* **2005**, *93*, S23.
11. Bird, B.; Swain, S. M. *Clin. Cancer Res.* **2008**, *14*, 14.
12. Ewer, M. S.; Gluck, S. *Cancer* **2009**, *115*, 1813.
13. Borisy, A. A.; Elliott, P. J.; Hurst, N. W.; Lee, M. S.; Lehar, J.; Price, E. R.; Serbedzija, G.; Zimmermann, G. R.; Foley, M. A.; Stockwell, B. R.; Keith, C. T. *Proc. Natl. Acad. Sci. U.S.A.* **2003**, *100*, 7977.
14. Kaufmann, M.; Jonat, W.; Hilfrich, J.; Eidtmann, H.; Gademann, G.; Zuna, I. *J. Clin. Oncol.* **2007**, *25*, 2664.

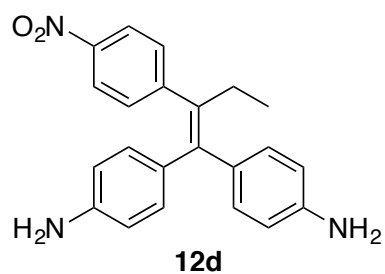
15. Boccardo, F.; Rubagotti, A.; Guglielmini, P.; Fini, A.; Paladini, G.; Mesiti, M.; Rinaldini, M.; Scali, S.; Porpiglia, M.; Benedetto, C.; Restuccia, N.; Buzzi, F.; Franchi, R.; Massidda, B.; Distante, V.; Amadori, D.; Sismondi, P.; trial, I. T. A. *Ann. Oncol.* **2006**, *17*, VIII10.
16. Baum, M.; Buzdar, A.; Cuzick, J.; Forbes, J.; Houghton, J.; Howell, A.; Sahmoud, T.; Group, A. T. *Cancer* **2003**, *98*, 1802.
17. Lu, W. J.; Xu, C.; Pei, Z. F.; Mayhoub, A. S.; Cushman, M.; Flockhart, D. A. *Breast Cancer Res. Treat.* **2012**, *133*, 99.
18. Lv, W.; Liu, J.; Lu, D.; Flockhart, D. A.; Cushman, M. *J. Med. Chem.* **2013**, *56*, 4611.
19. Lv, W.; Liu, J. Z.; Skaar, T. C.; Flockhart, D. A.; Cushman, M. *J. Med. Chem.* **2015**, *58*, 2623.
20. Lv, W.; Liu, J.; Skaar, T. C.; O'Neill, E.; Yu, G.; Flockhart, D. A.; Cushman, M. *J. Med. Chem.* **2016**, *59*, 157.
21. Haynes, B. P.; Dowsett, M.; Miller, W. R.; Dixon, J. M.; Bhatnagar, A. S. *J. Steroid Biochem. Mol. Biol.* **2003**, *87*, 35.
22. Gobbi, S.; Zimmer, C.; Belluti, F.; Rampa, A.; Hartmann, R. W.; Recanatini, M.; Bisi, A. *J. Med. Chem.* **2010**, *53*, 5347.
23. Detsi, A.; Koufaki, M.; Calogeropoulou, T. *J. Org. Chem.* **2002**, *67*, 4608.
24. Yu, D. D.; Forman, B. M. *J. Org. Chem.* **2003**, *68*, 9489.
25. Uddin, M. J.; Rao, P. N. P.; Knaus, E. E. *Bioorg. Med. Chem.* **2004**, *12*, 5929.
26. Nenajdenko, V. G.; Lenkova, O. N.; Shastin, A. V.; Balenkova, E. S. *Synthesis* **2004**, 573.

27. Korotchenko, V. N.; Shastin, A. V.; Nenajdenko, V. G.; Balenkova, E. S. *J. Chem. Soc. Perkin Trans. 1* **2002**, 883.
28. Ghosh, D.; Lo, J.; Morton, D.; Valette, D.; Xi, J.; Griswold, J.; Hubbell, S.; Egbuta, C.; Jiang, W.; An, J.; Davies, H. M. L. *J. Med. Chem.* **2012**, *55*, 8464.
29. Shiau, A. K.; Barstad, D.; Loria, P. M.; Cheng, L.; Kushner, P. J.; Agard, D. A.; Greene, G. L. *Cell* **1998**, *95*, 927.
30. Lu, W. J.; Desta, Z.; Flockhart, D. A. *Breast Cancer Res. Treat.* **2012**, *131*, 473.
31. Lim, Y. C.; Desta, Z.; Flockhart, D. A.; Skaar, T. C. *Cancer Chemother. Pharmacol.* **2005**, *55*, 471.
32. Liu, J. Z.; Flockhart, P. J.; Lu, D. S.; Lv, W.; Lu, W. J. J.; Han, X.; Cushman, M.; Flockhart, D. A. *Drug Metab. and Dispos.* **2013**, *41*, 1715.
33. Paruthiyil, S.; Parmar, H.; Kerekatte, V.; Cunha, G. R.; Firestone, G. L.; Leitman, D. C. *Cancer Res.* **2004**, *64*, 423.
34. Lee, K. J.; Kim, J. L.; Hong, M. K.; Lee, J. Y. *J. Heterocycl. Chem.* **1999**, *36*, 1235.
35. Agouridas, V.; Laios, I.; Cleeren, A.; Kizilian, E.; Magnier, E.; Blazejewski, J.-C.; Leclercq, G. *Bioorg. Med. Chem.* **2006**, *14*, 7531.
36. Shoda, T.; Okuhira, K.; Kato, M.; Demizu, Y.; Inoue, H.; Naito, M.; Kurihara, M. *Bioorg. Med. Chem. Lett.* **2014**, *24*, 87.
37. Arsenyan, P.; Paegle, E.; Domracheva, I.; Gulbe, A.; Kanepė-Lapsa, I.; Shestakova, I. *Eur. J. Med. Chem.* **2014**, *87*, 471.
38. Ohta, K.; Chiba, Y.; Kaise, A.; Endo, Y. *Bioorg. Med. Chem.* **2015**, *23*, 861.

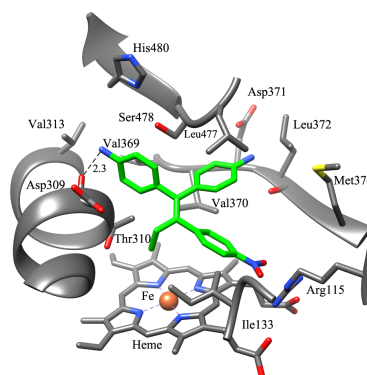
39. Shoda, T.; Kato, M.; Harada, R.; Fujisato, T.; Okuhira, K.; Demizu, Y.; Inoue, H.; Naito, M.; Kurihara, M. *Bioorg. Med. Chem.* **2015**, *23*, 3091.

ACCEPTED MANUSCRIPT

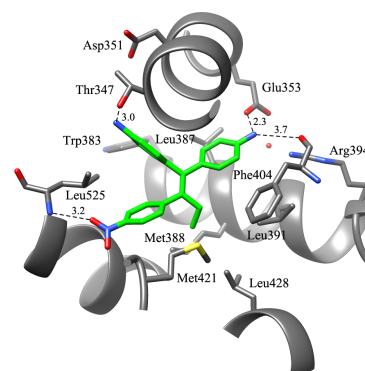
Graphical Abstract



Aromatase $\text{IC}_{50} = 62.2 \text{ nM}$
ER- α $\text{EC}_{50} = 72.1 \text{ nM}$
ER- β $\text{EC}_{50} = 70.8 \text{ nM}$



12d + Aromatase



12d + ER- α

ACCEPTED MANUSCRIPT